Influence of Lipid Chemistry on Membrane Fluidity: Tail and Headgroup Interactions

Kalani J. Seu, Lee R. Cambrea, R. Michael Everly, and Jennifer S. Hovis
Department of Chemistry, Purdue University, West Lafayette, Indiana

ABSTRACT Membrane fluidity plays an important role in cell function and may, in many instances, be adjusted to facilitate specific cellular processes. To understand better the effect that lipid chemistry has on membrane fluidity the inclusion of three different lipids into egg phosphatidylcholine (eggPC) bilayers has been examined; the three lipids are egg phosphatidylethanolamine ((eggPE) made by transphosphatidylation of eggPC in the presence of ethanolamine), lyso-phosphatidylcholine (LPC), and lyso-phosphatidylethanolamine (LPE). The fluidity of the membranes was determined using fluorescence recovery after photobleaching and the intermolecular interactions were examined using attenuated total reflection Fourier transform infrared spectroscopy. It was observed that both headgroup and tail chemistry can significantly modulate lipid diffusion. Specifically, the inclusion of LPC and eggPE significantly altered the lipid diffusion, increased and decreased, respectively, whereas the inclusion of LPE had an intermediate effect, a slight decrease in diffusion. Strong evidence for the formation of hydrogen-bonds between the phosphate group and the amine group in eggPE and LPE was observed with infrared spectroscopy. The biological implications of these results are discussed.

INTRODUCTION

Lipid fluidity is a distinctive feature of cell membranes. The presence of lipids undergoing long-range diffusion is a good test of membrane integrity and is believed to play a crucial role in many cellular processes including the facilitation of cell signaling (1), cell adhesion (2–4), and enzyme binding/activity (5). Lipid fluidity also plays an important part in the resistance of microorganisms (6) and plants (7,8) to environmental stresses, e.g., freezing and dehydration. Plants, for instance, will alter their membrane composition as a means of optimizing membrane fluidity (7,8). The extent to which different lipids modulate fluidity is therefore of considerable interest.

The diffusion of lipids in model membranes and cells has been measured numerous times (9–18). The local environment can be probed with fluorescence techniques, such as single fluorescent molecule video imaging (SFVI) and single particle tracking (SPT). The long-range diffusion can be probed with fluorescence correlation spectroscopy (FCS), fluorescence recovery after photobleaching (FRAP), and nuclear magnetic resonance (NMR). Despite considerable use of these techniques, there are few systematic studies examining the effect of lipid chemistry on membrane fluidity. Systematic fluidity studies are necessary because single measurements from different articles can rarely be compared; for instance, lipids in monolayers diffuse faster than those in bilayers (19) and lipids in bilayers on solid supports diffuse differently depending on the nature of the support (K. Seu and J. Hovis, unpublished data). To our knowledge, the effect of only cholesterol and sphingomyelin (SM) on long-range diffusion has been studied in a rigorously systematic manner, both of which change the lipid diffusion in phosphatidylcholine (PC) bilayers (12,14,21–28).

In this article the effect that three different lipids, phosphatidylethanolamine (PE), lyso-phosphatidylethanolamine (LPE), and lyso-phosphatidylcholine (LPC), have on diffusion in PC bilayers will be examined (lyso refers to a single-tailed lipid). Structures of these lipids are shown in Fig. 1. These lipids are biologically interesting as PC and PE are the two most commonly occurring zwitterionic lipids in mammalian cells whereas lyso lipids can be created in the membrane by phospholipase A2 (PLA2) and may therefore be important in the cellular modulation of lipid fluidity. The lipids are also interesting from a fundamental perspective as they afford the opportunity to examine the influence of both headgroup and tail chemistry on lipid diffusion. Fluorescence recovery after photobleaching will be used to determine the diffusion coefficients. The experimental setup was constructed to ensure that the measurements stay within the constraints of theory, as will be discussed. Determining the factors that influence lipid diffusion is difficult due to the lack of both good models and complimentary experimental data. To confirm/validate theoretical models, experimental measurements are needed; this article will add significantly to the available diffusion measurements. To further assist in both interpreting the diffusion data and developing models, we examined the lipids with attenuated total reflection Fourier transform infrared spectroscopy (ATR-FTIR), which gives information about specific intermolecular interactions. It will be shown that both headgroup and tail chemistry have a significant effect on lipid diffusion and that the changes observed can be attributed to alterations in membrane height, van der Waals interactions, and hydrogen-bonding.

Submitted March 7, 2006, and accepted for publication August 16, 2006.

Address reprint requests to Jennifer S. Hovis, Tel.: 765-494-4115; Fax: 765-494-0239; E-mail: jhovis@purdue.edu.

0006-3495/06/11/3727/09 $2.00

doi: 10.1529/biophysj.106.084590

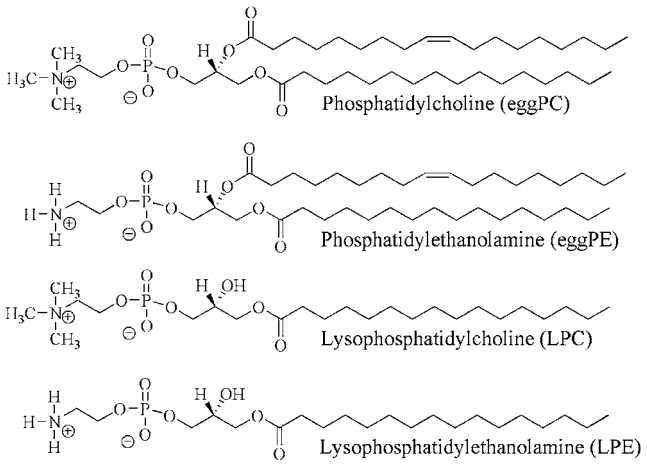

FIGURE 1 Chemical structures of the investigated lipids: L-α-phosphatidylcholine (eggPC), L-α-phosphatidylethanolamine (eggPE), lyso-phosphatidylcholine (LPC), and lyso-phosphatidylethanolamine (LPE). Note that eggPC is extracted from chicken eggs and eggPE is made by the transphosphatidylation of eggPC in the presence of ethanolamine; therefore both lipids have a distribution of fatty acid chains, the most common of which are drawn here.

MATERIALS AND METHODS

Materials

Chloroform solutions of L-α-phosphatidylcholine from egg (eggPC), L-α-phosphatidylethanolamine made by transphosphatidylation of egg lectin in the presence of ethanolamine (eggPE), 1-palmitoyl-2-hydroxy-*sn*-glycero-3-phosphocholine (LPC), L-α-lysophosphatidylethanolamine from egg (LPE), and 1-oleoyl-2-[6-[(7-nitro-2-1,3-benzoxadiazol-4-yl)amino]hexanoyl]-*sn*-glycero-3-phosphocholine (NBD-PC) were purchased from Avanti Polar Lipids (Birmingham, AL) and were used without further purification. The (*N*-[2-hydroxyethyl]piperazine-*N*′-[2-ethanesulfonic acid]) (HEPES) and ethylenediaminetetraacetic acid (EDTA) were purchased from Sigma Chemical (St. Louis, MO). Spectrophotometric grade cholorform was purchased from Mallinkrodt (St. Louis, MO). ICN 7X detergent was purchased form ICN (Costa Mesa, CA). Glass slides, 22 × 30 No. 1.5, were purchased from Fisher Scientific (Hanover Park, IL). Double-side polished silicon (001) wafers (>10Ω-cm resistivity, ~525 μm thick) for making ATR elements were purchased from Silicon (Boise, ID). The buffer used in the experiments, 100 mM NaCl, 50 mM HEPES, 0.1 mM EDTA, was adjusted to pH 7.4 using 1 M NaOH.

Vesicle preparation

Mixtures of different lipids at appropriate molar ratios in chloroform were dried under nitrogen and held under vacuum for 1 h; the dried lipids were resuspended in 18 MΩ-cm water. Large unilamellar vesicles (LUVs) were prepared by extruding the lipid suspension through polycarbonate membranes, with 50 nm pores, a minimum of 21 times. The resulting LUVs were then centrifuged for 5 min at 14,000 rpm (Eppendorf Minispin Plus, Westbury, NY).

Supported lipid bilayers

Supported lipid bilayers were formed by vesicle fusion on glass surfaces.(29,30) Briefly, 60 μL of a 1:1 vesicle/buffer solution was injected into a CoverWell perfusion chamber gasket (Molecular Probes, Eugene, OR) adhered to a glass coverslip (Fisher Scientific). The perfusion chamber gasket creates a sealed chamber to contain the vesicle solution, on the highly hydrophilic glass coverslip, during the fusion process. The coverslips were prepared by washing in dilute ICN 7X detergent (VMR International, Chicago, IL), rinsing exhaustively in distilled water, drying with nitrogen and baking at 450°C for 4 h. Excess vesicles were removed by submerging the coverslip in 18 MΩ-cm water, removing the gasket, and shaking gently for ~15 s; this yielded uniform fluid membrane-covered surfaces. Samples were sandwiched using a coverslip, placed on a homebuilt Delrin sample holder, and kept fully hydrated, using 18 MΩ-cm water, during analysis.

Fluorescence recovery after photobleaching (FRAP)

Supported lipid bilayers were formed by vesicle fusion on appropriately treated glass slides. A Nikon TE2000-U fluorescence microscope equipped with a 40×/1.30 N.A. oil immersion objective, an NBD filter set (Chroma Technology, Brattleboro, VT), and a silicon avalanche photodiode (APD) Single Photon Counting Module (SPCM-AQR-16-FC, PerkinElmer, Vaudreuil, Quebec) was used to focus, collect, and count the emitted fluorescence. A 25 mW Argon ion laser (488 nm Melles Griot, Carlsbad, CA) was used to both bleach and monitor the lipid bilayer. The bleach spot radius was 10.6 μm and the quality of the spot was checked by acquiring images of dilute calcein with a Cascade 650 CCD camera (Photometrics, Roper Scientific, Tucson, AZ). The bilayers were bleached to background levels in 1 s: this is ~0.3% of the total recovery time. To reduce further bleaching of the fluorophore during the recovery period the laser intensity was reduced 100,000-fold using a 5× (focal transmission of 1×10^5) neutral density filter (NE50B, Thorlabs, Newton, NJ). Before bleaching, the sample was monitored a minimum of 40 s to determine the initial fluorescence intensity; at this reduced laser power the sample can be monitored without a drop in bilayer intensity. An automated neutral density filter (74041, Oriel Instruments, Stratford, CT) is used to move the filter in and out of the beam path. A LabVIEW program was used to acquire the counts from the APD, control the filter wheel, and trigger the shutter (Uniblitz, Rochester, NY). The fitting of FRAP data to obtain a diffusion coefficient has been discussed in detail elsewhere (31,32). Diffusion coefficients (D) were determined by fitting the fluorescence recovery curve to the solution of the differential equation for lateral transport of a molecule undergoing Brownian motion (31), using the method of Soumpasis (32). All experiments were conducted at 22°C and the percent fluorescent recovery measured for all experiments was ≥95% (In examining hundreds of recovery curves we observed that recoveries <95% resulted in poor fits to the data; the amount of recovery is therefore a useful criterion for the quality of the data.).

Attenuated total reflection-Fourier transform infrared spectroscopy (ATR-FTIR)

A Nicolet 470 FTIR equipped with a mercury cadmium telluride type A (MCTA*) detector was used to collect the spectra. A homebuilt ATR setup was used, as described in detail elsewhere (33). In brief, IR light is sent out of the spectrometer and coupled into an ATR element, created in-house, (15 mm × 9 mm × 525 μm silicon wafer) at 45°. Before introducing the lipids, a background of the silicon ATR element and the buffer was collected. To form supported lipid bilayers, LUVs were injected into one side of the custom-made Delrin flow-cell (10 μL) and allowed to incubate for 30 min. Once the bilayer had formed, buffer was flushed through the flow-cell to rinse away excess vesicles and the sample spectrum was obtained and ratioed against the background spectra. For both the background and sample spectra, 1600 scans were signal averaged at a resolution of 4 cm^{-1} using Happ-Genzel apodization and zero filling.

RESULTS

Determining diffusion coefficients by fluorescence recovery after photobleaching

In fluorescence recovery after photobleaching, fluorophores in a defined region are bleached and the movement of either

the bleached fluorophores out of the spot or the movement of the unbleached fluorophores into the spot is monitored. The use of FRAP to determine the diffusion coefficient of lipids in membranes was pioneered by Axelrod et al. (31) who showed that by monitoring the diffusion of fluorescent lipids into the bleach spot, while knowing the beam waist and bleach laser intensity, the diffusion coefficient of the labeled lipids could be obtained. By recasting the problem, Soumpasis (32) was able to remove the need to know the bleach laser intensity; the treatments developed therein have become the standard methods for determining lipid diffusion. Soumpasis describes two ways in which diffusion coefficients can be obtained from the intensity of the fluorescence, within the bleach spot, with respect to time. The first, less accurate, method involves using a least squares fit of a single exponential to the aforementioned fluorescence recovery data to determine the time to half fluorescence intensity recovery ($t_{1/2}$), and then calculating the diffusion coefficient with the following:

$$D = 0.224\frac{w^2}{t_{1/2}}, \tag{1}$$

where w is the radius of the circular bleach beam. The second, more accurate and rigorous, method involves fitting the fluorescence recovery data to:

$$f(t) = e^{(-2\tau_D/t)}[I_o(2\tau_D/t) + I_1(2\tau_D/t)], \tag{2}$$

where τ_D is the characteristic diffusion time and I_0 and I_1 are modified Bessel functions. The diffusion coefficient can then be determined from τ_D using:

$$D = \frac{w^2}{4\tau_D}. \tag{3}$$

In both methods it is assumed that the recovery is complete.

A significant challenge in acquiring FRAP data is eliminating unwanted photobleaching while monitoring the fluorescence recovery. To avoid this problem the laser used for monitoring the recovery is attenuated to 250 nW (this is a 100,000-fold decrease in intensity from that used to bleach the sample, 25 mW). At this laser power the sample can be monitored indefinitely with no observable change in fluorescence intensity. Fig. 2 shows a typical FRAP recovery curve for an eggPC supported lipid bilayer containing 0.5 mol % NBD-PC along with two fits to the data—a least squares fit of a single exponential (the less accurate method) and a least squares fit to Eq. 2. For this data set the diffusion coefficient determined using the exponential fit is 1.8 $\mu m^2/s$, and using Eq. 2 is 2.4 $\mu m^2/s$. Before the bleach ($t = 0$) data points are collected to obtain the initial fluorescence intensity of the bilayer; these values are then averaged and used to normalize the data. It is clear that the fit to the exponential is poor, showing a deviation from the data at both the curved and the tail regions of the recovery, whereas the fit to Eq. 2 is excellent. The quality of the fit to both equations can further

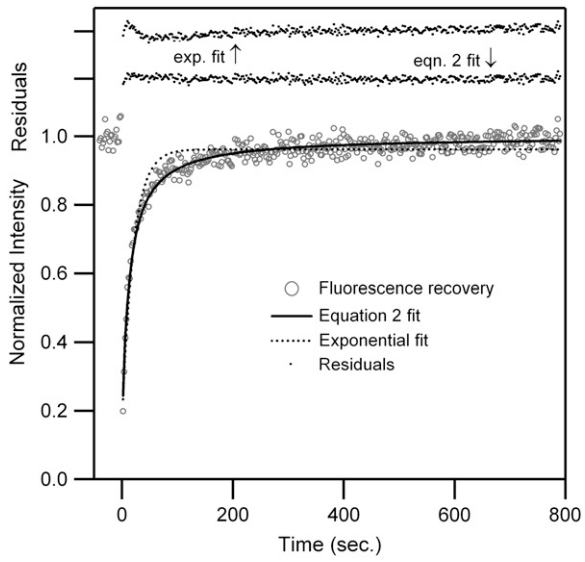

FIGURE 2 Typical FRAP recovery curve for an eggPC supported lipid bilayer containing 0.5 mol % NBD-PC along with a least squares fit of a single exponential and a least squares fit to Eq. 2. Photons are counted for 1 s every other second. Residuals for both fit functions are displayed at the top. The exponential fit shows a deviation from the data at both the curved and the tail regions of the recovery, whereas the residuals from the fit to Eq. 2 show no deviations.

be seen in the residuals, which are plotted at the top of Fig. 2. From our experience, the exponential fit almost always returns lower diffusion coefficients than those obtained by using Eq. 2. As the exponential fit is commonly used to determine diffusion coefficients, we have examined the two fits in more detail. In general, the diffusion coefficient values returned by the exponential fit vary significantly depending on the sampling rate and the amount of time the recovery is monitored, in contrast the values returned using Eq. 2 are largely insensitive to these variables.

To examine the effect that different lipids have on diffusion, it is necessary to first determine how many times a particular composition needs to be interrogated; i.e., what is the error in a given measurement? In considering supported lipid bilayers, three possibilities for repeated interrogation are apparent: 1) the same spot is bleached multiple times; 2) vesicle preparations on different days are bleached; and 3) different spots on the same slide are examined. Table 1 shows the results from bleaching the same spot, on an eggPC bilayer with 0.5 mol % NBD-PC, multiple times. Within a given spot the error varies from ~5–15%.

The large error in diffusion, within a single spot, was initially surprising. Some of this variation is certainly due to the inherent noise level in the measurement, whereas some may be due to drift in the microscope stage. Increasing the probe concentration or using a more sensitive detector would help to reduce the variation; the downside of increasing the probe concentration is that it increases the perturbations to the system of interest, resulting in data that is not as representative

TABLE 1 Diffusion results from bleaching the same composition multiple times

Vesicle preparation	Bleach no.	D ($\mu m^2/s$)	Average D within preparation	Weighted average
First	1	2.070	2.19 ± 0.12	2.5 ± 0.1 $\mu m^2/s$
	2	2.176	(5.6% error)	(4% error)
	3	2.139		
	4	2.358		
Second	1	2.374	2.67 ± 0.33	
	2	2.607	(12% error)	
	3	2.564		
	4	3.155		
Third	1	2.999	2.90 ± 0.21	
	2	2.662	(7.3% error)	
	3	3.067		
	4	2.970		
Fourth	1	2.957	2.80 ± 0.13	
	2	2.640	(4.7% error)	
	3	2.834		
	4	2.752		

Diffusion results from bleaching a single spot, four consecutive times, for an eggPC bilayer with 0.5 mol % NBD-PC. Data from four different preparations are combined to obtain diffusion coefficients via a weighted average.

of the lipids being investigated. In Table 1 the variation from one preparation to the next can also be seen, again a significant change is observed; this variation is probably due to slight compositional changes and alterations in the surface chemistry of the solid support. The slides used in this study were baked and used within 24 h. In our experience baked slides are ''good'' for only a few days after baking; it is difficult to consistently form uniform fluid bilayers on baked slides that are more than a few days old, indicating that some change occurs to the surface chemistry and/or the morphology with time. As both the composition and support should be more uniform across a single sample, than from one sample to another, it was decided that pursuing the third possibility, examining different spots on the same sample, would not lend any additional insight and might result in the misrepresentation of the true compositional variance of the measurement, so this approach was not applied.

To compute the diffusion coefficient for a given composition the following was done: 1) In a single spot, for a given sample, a series of four consecutive FRAP experiments were conducted (data were rejected if reduced χ^2 values from the fitted function were >1). 2) The values from the single spot were averaged together and an error for the measurement was determined by calculating the standard deviation of the mean. 3) Data from different preparations were then combined to obtain diffusion coefficients via a weighted average. As can be seen in Table 1, there is quite a bit of variation both within a spot and from sample to sample; consequently if the variation due to changes in composition is small it may not be observable unless multiple measurements are made. Therefore, a single diffusion data point reported in this article contains anywhere from 7 to 16 individual FRAP measurements.

Effect of composition on measured diffusion coefficient

In Fig. 3 the normalized diffusion coefficients are shown for varying concentrations of LPC, LPE, and eggPE lipids in eggPC. Diffusion coefficients are normalized using the diffusion coefficient obtained for 100 mol % eggPC bilayers; this was done to make it easier to see the extent to which the various lipids affect the diffusion coefficient. The eggPE was made by transphosphatidylation of eggPC in the presence of ethanolamine; as a result the tail composition of eggPE is the same as that of eggPC. Vesicles were made by extrusion (labeled with 0.5 mol % NBD-PC) and fused to treated glass supports, as detailed in the Materials and Methods section, to form planar supported lipid bilayers.

The open squares in Fig. 3 show the incorporation of 0, 10, 20, and 30 mol % LPC into eggPC bilayers. It was not possible to form vesicles containing 40 mol % or greater of LPC (34). There is a large linear increase in the diffusion coefficient as LPC is incorporated into eggPC bilayers. The diffusion increases by ~97% with the incorporation of 30 mol % LPC; by fitting the data it can be determined that to increase the lipid diffusion by ~10% only 3 mol % LPC is needed, a substantial change for a small alteration in composition. The effect of the addition of 0, 20, 40, 60, and 80 mol % LPE into eggPC bilayers is shown in Fig. 3 (*open triangles*). As compared with LPC the incorporation of LPE has a smaller effect on lipid diffusion. The diffusion coefficient stays fairly constant with a slight downward (decreasing) trend as LPE is added; the incorporation of 80 mol % LPE reduces the lipid diffusion by ~37%. The incorporation

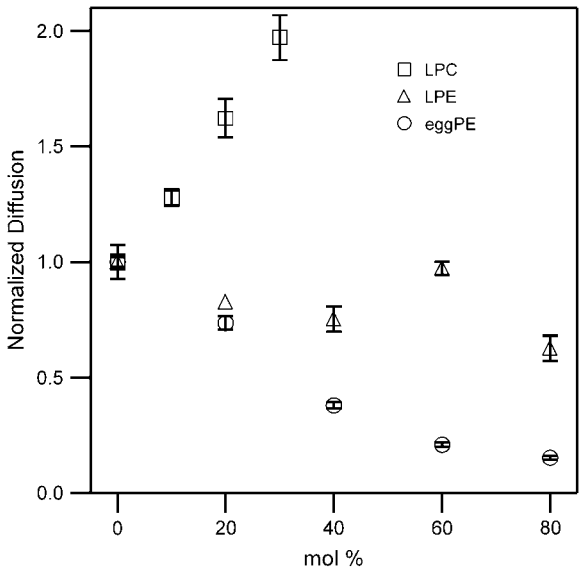

FIGURE 3 Normalized diffusion coefficients for varying concentrations of LPC (□), LPE (△), and eggPE (○) lipids in eggPC. Diffusion coefficients are normalized using the diffusion coefficient obtained for 100 mol % eggPC bilayers. For clarity, the error bar on the 20 mol % LPE (±0.03) has been removed.

of 0, 20, 40, 60, and 80 mol % eggPE is also shown in Fig. 3 (*open circles*). The inclusion of eggPE results in a decrease in the diffusion coefficient. This decrease in diffusion is initially linear and then it plateaus around 60 mol % eggPE. Overall the diffusion decreases by ~85% when 80 mol % eggPE has been added to the eggPC bilayer. The drop is most significant from 0 to 40 mol % eggPE; in this regime the lipid diffusion decreases by ~10% when there is a 7.5 mol % change in eggPE composition.

Evidence for hydrogen-bonding between lipids

To assist in determining the factors that caused the observed changes in diffusion we have examined the lipid mixtures with ATR-FTIR; all three of the lipids added to eggPC contain hydrogen-bond donating group. Hydrogen-bonding is a strong intermolecular force and so the question arises as to whether it affects lipid diffusion. The donating groups in these lipids are as follows: eggPE, N−H; LPE, N−H and O−H; LPC, O−H. We have recently shown that infrared spectroscopy can be done on single fluid lipid bilayers (FRAP can be done after spectra are acquired to confirm fluidity) (33). As spectroscopy provides a direct method to probe hydrogen-bonding, IR spectra were acquired of single lipid bilayers on silicon ATR crystals, as previously described (33); see Fig. 4 for an example. From an intermolecular interactions perspective, the peaks of interest arise from the following three functional groups: the carbon-hydrogen bonds, the carbonyl group, and the phosphate group. The C−H stretching region is sensitive to tail packing and the ν(C=O) and $\nu_{as}(PO_2^-)$ are sensitive to their hydrogen-bonding environment; the effect that the incorporation of eggPE, LPC, and LPE has on each group will be discussed in turn.

In all mixtures examined in this work no peak shifts were observed in the C−H stretching region. The transition from the gel-to-fluid phase, which causes a change in diffusion of two orders of magnitude (35), leads to only a 5 cm^{-1} shift in the position of the $\nu_s(CH_2)$ and $\nu_{as}(CH_2)$ bands (36). Given the resolution of the spectra (4 cm^{-1}) and that the diffusion changes in these mixtures by less than an order of magnitude, it is not surprising that no alterations with composition are seen in the C−H stretching region.

In Fig. 5 the $\nu_{as}(PO_2^-)$ region is shown for eggPC bilayers containing eggPE, LPE, and LPC. Unfortunately, the $\nu_s(PO_2^-)$

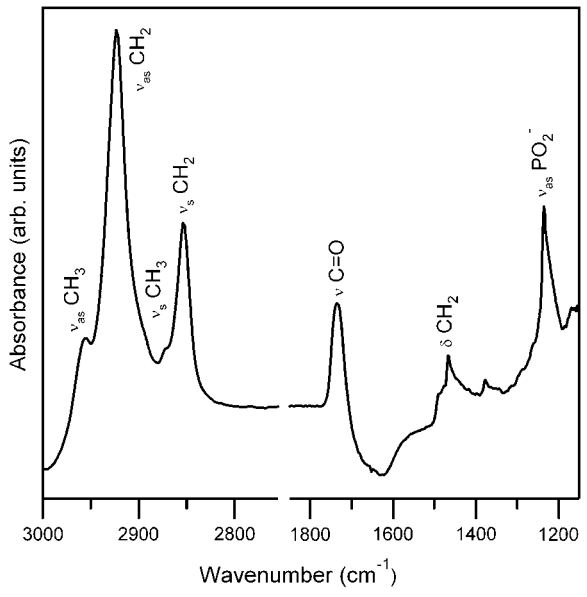

FIGURE 4 IR spectra of an eggPC lipid bilayer on a silicon ATR crystal. Peaks of interest have been labeled. The dip centered at ~1645 cm^{-1} is due to the water bending region.

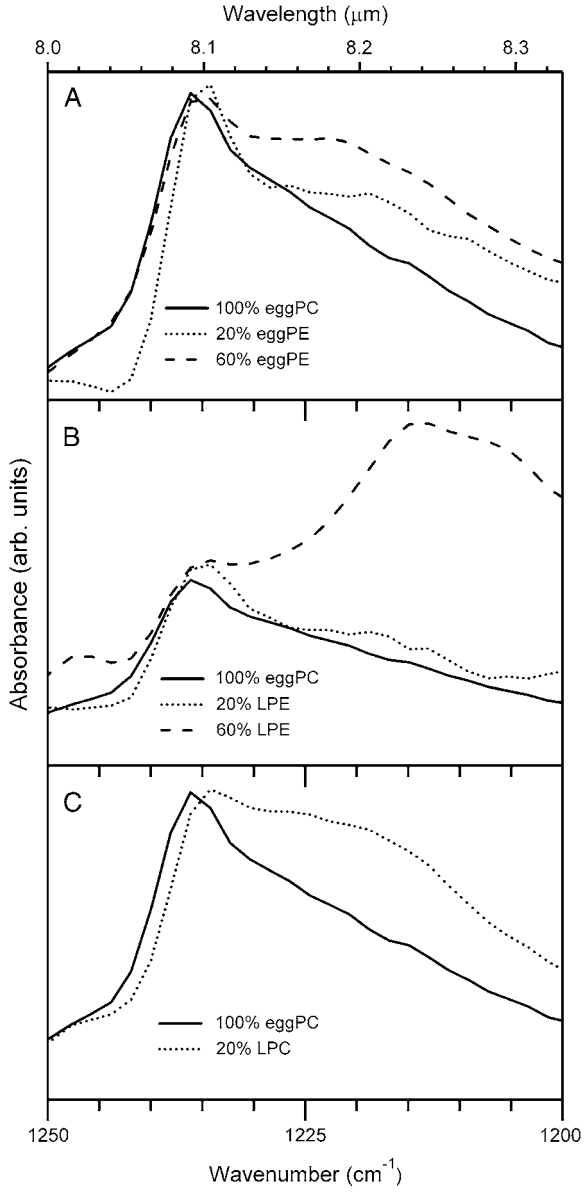

FIGURE 5 The $\nu_{as}(PO_2^-)$ region from ATR-FTIR spectra of eggPC bilayers containing varying concentrations of (*A*) eggPE, (*B*) LPE, and (*C*) LPC.

region (1085 cm^{-1}) overlaps with the near total absorption by the silicon crystal (~1100 cm^{-1}) and consequently cannot be observed. In Fig. 5 *A* it can be seen that the phosphate peak shifts to lower wavenumbers (red-shifts) upon the incorporation of eggPE lipids. Previous work has shown that as the phosphate group in anhydrous PC becomes hydrated, the $\nu_{as}(PO_2^-)$ shifts to lower wavenumbers (37–39). It is also known that PE headgroups are less hydrated than PC headgroups (40–42). Thus, one would predict that the inclusion of eggPE lipids would shift $\nu_{as}(PO_2^-)$ to higher wavenumbers, yet the opposite is observed. We suggest that the red shift arises from the formation of intermolecular hydrogen-bonds between the eggPE amine group and the phosphate group; the amine absorption is in the same region as water and cannot be observed. Spectra taken of dry PC and PE lipids also showed a red shift of the PE phosphate relative to the PC phosphate and this shift was ascribed to hydrogen-bonding between the amine and the phosphate (43,44).

With the incorporation of LPE the phosphate again red-shifts, Fig. 5 *B*. In this case, the shift is particularly dramatic when 60 mol% LPE is incorporated; the lack of bulk in the tail region may make it easier for LPE to form intermolecular hydrogen-bonds than eggPE. LPE is the one lipid that contains two donating groups. Part of the shift could be attributable to hydrogen-bonding with the −OH group; this group absorbs in the water region and consequently cannot be seen. As with eggPE and LPE, the incorporation of LPC also resulted in a red shift of the phosphate group, fig. 5C. This suggests that the –OH group is able to interact with the phosphate; as will be seen when examining the carbonyl region, it appears that the lyso lipids have considerable flexibility in their motion, therefore it is not unreasonable for hydrogen-bonding to occur between the two groups.

The ν(C=O) region from eggPC bilayers containing eggPE, LPE, and LPC is shown in Fig. 6. The slight asymmetry of the ν(C=O) peak is due to it being located near the strong absorption of water due to bending modes, $\delta(H_2O)$ centered at ~1645 cm^{-1}. In all spectra shown, the background spectra are of buffer. When a bilayer is formed, by vesicle fusion, on the ATR element the lipids displace water; consequently, there is an increase in all of the lipid associated peaks (e.g., $\nu(CH_2)$, ν(C=O), etc.) and a decrease in the water associated peaks ($\delta(H_2O)$ and $\nu(H_2O)$). Thus, the side of the ν(C=O) nearest to the water bending region (~1645 cm^{-1}) appears to dip lower. For fully hydrated diacyl PCs, a single broad carbonyl peak centered around 1730 cm^{-1} is observed (45). This broad carbonyl peak is composed of two separate components: a ''dehydrated'' carbonyl (~1740 cm^{-1}) and a ''hydrated'' carbonyl (~1727 cm^{-1})—corresponding to the *sn-1* and *sn-2* carbonyl groups, respectively (46). As with the phosphate group, the carbonyl group shifts to lower wavenumber (red shifts) with increasing hydration.

In Fig. 6 *A* the carbonyl region is shown for eggPC bilayers containing varying amounts of eggPE. The incorporation of eggPE into eggPC bilayers has no observable effect

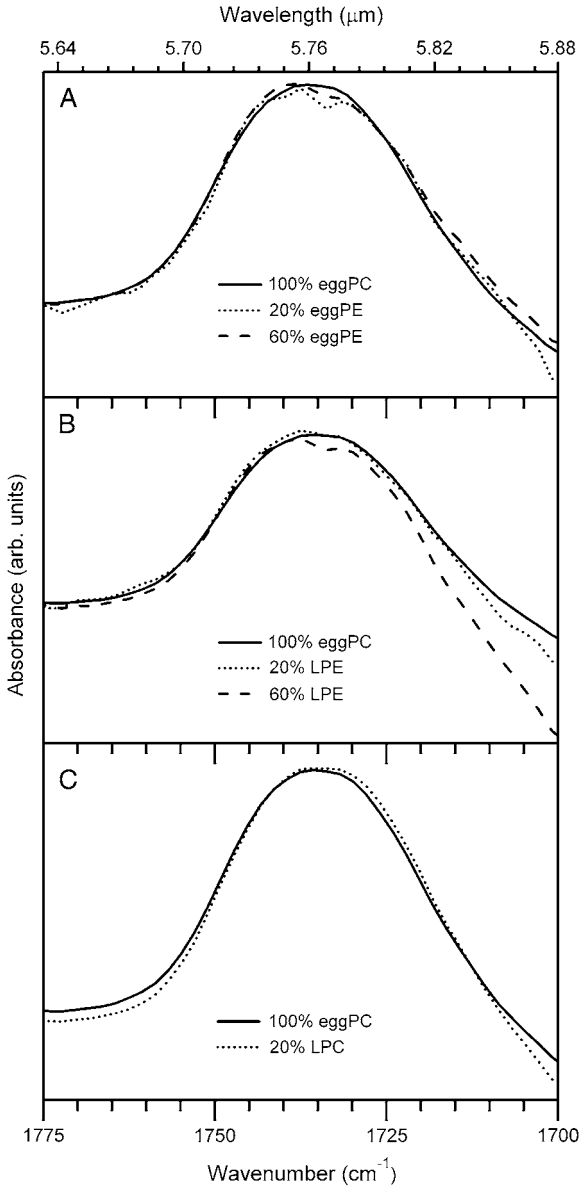

FIGURE 6 The ν(C=O) region from ATR-FTIR spectra of eggPC bilayers containing varying concentrations of (*A*) eggPE, (*B*) LPE, and (*C*) LPC.

on the carbonyl group—because eggPE headgroups are less hydrated this is somewhat surprising. As with the phosphate, it could be that the lower degree of hydration is balanced by intermolecular hydrogen-bonding; sterically it would be more difficult for the amine to hydrogen-bond with the carbonyl, as opposed to the phosphate, but not impossible. Interestingly, the incorporation of LPE or LPC into eggPC bilayers also has little effect on the carbonyl region, Fig. 6, *B* and *C*. The lyso lipids contain only a single carbonyl group, the *sn-1* carbonyl, which has been assigned as the ''dehydrated'' group; therefore the carbonyl peak would have been expected to be blue-shifted upon incorporation of the lyso lipids. The lack of change indicates either that the lyso lipids

are more free to sample a variety of environments; i.e., their up and down motion is more significant than the two tailed lipids, or that hydrogen-bonding is occurring between the carbonyl and the donating groups.

DISCUSSION

The results in Fig. 3 clearly show that both headgroup chemistry and tail chemistry have a significant effect on lipid diffusion. To examine the origin of the changes observed in the figure, diffusion in two dimensions is considered. Diffusion in three dimensions can be related to particle area, viscosity, and temperature; in two dimensions, however, there is no solution to the viscous-flow equations for an infinite membrane, the Stokes paradox. Various groups have shown that making a variety of different assumptions can circumvent the paradox. For lipid diffusion a free area model is typically used,(47,48)

$$D_{\mathrm{T}} \sim \exp(-a_{\mathrm{o}}/a_{\mathrm{f}}), \tag{4}$$

where a_{o} is an estimate for the average cross-sectional area and a_{f} is a measure for the average amount of free area per molecule in the bilayer. With regards to using the free-area model the problem of how to define the free-area immediately arises (25,49,50). This is particularly evident in considering the incorporation of LPC into eggPC; there, the change in free-area likely varies significantly with depth. The other main membrane model is Saffman-Delbrück (51); there the outer liquid (bulk water) is given a finite viscosity,

$$D = \frac{k_{\mathrm{B}}T}{4\pi\eta h}\left(\log\frac{\eta h}{\eta' a} - \gamma\right), \tag{5}$$

where η is the membrane viscosity, η' the outer liquid viscosity, h the membrane height, a the particle area, T the temperature, and γ Euler's constant. The Saffman-Delbrück model has more commonly been used for protein diffusion; given the problems associated with the free area model we have reexamined Saffman-Delbrück and will show that it allows for significant insight into the factors that contribute to the observed changes in diffusion.

In the Saffman-Delbrück model, diffusion has a weak dependence on lipid area and a strong inverse dependence on membrane viscosity and lipid height. Viscosity is a measure of the strength of the intermolecular interactions; the interactions that hold lipids together include van der Waals interactions, hydrogen-bonding, and screened electrostatic. Both van der Waals forces and hydrogen-bonding interactions should be significant; in DPPC the average energy per CH_2 group has been estimated to be 2.1 kJ/mol; multiplying by 16 gives 33.6 kJ/mol for a single lipid tail (52) whereas hydrogen-bonds are estimated to be ~10–40 kJ/mol (52). Screened electrostatic interactions are probably comparatively less important, as all of the lipids are zwitterions. For each of the lipids incorporated into eggPC we will consider the effect of height, van der Waals interactions, and hydrogen-bonding.

Upon incorporation of eggPE into eggPC a significant decrease in diffusion was observed and this decrease was nonlinear in nature. In simulations, when PE is incorporated into PC bilayers a small increase in bilayer thickness is observed (53); the increase observed was ~15% from pure PC to pure PE and was roughly linear with PE content. From 0 to 80 mol % eggPE we observe a decrease of ~85% in the diffusion coefficient. Change in height therefore accounts for part of the decrease in diffusion; it does not, however, explain the nonlinear nature of the drop. The headgroup area of PE is smaller than that of PC, as a result the more PE that is present, the closer the tails are, the greater the van der Waals interactions, and the slower the diffusion. Regarding the nonlinearity of the drop, it is noted that by several experimental and computation methods a very similar decrease has been observed in the area per lipid as the amount of PE is increased in PC membranes (54–58); Fig. 3 in de Vries et al. (58) shows a comparison of these results. This strongly suggests that van der Waals interactions play a significant role in the observed changes in diffusion. Finally, infrared spectroscopy showed that eggPE is forming hydrogen-bonds with neighboring lipids, thus hydrogen-bonding also contributes to the decrease in diffusion coefficient. Height, van der Waals interactions, and hydrogen-bonding all contribute to the decrease in diffusion observed when eggPE is incorporated into eggPC; as to the relative contributions, van der Waals interactions contribute more than height. To assess the extent of the hydrogen-bonding contribution requires more information. Clearly, headgroup chemistry can have a large effect on lipid diffusion.

When LPC was incorporated into eggPC a large linear increase in the diffusion coefficient was observed. The tail chemistry of the LPC used in these experiments was 16:0 whereas the primary saturated tails in eggPC are 16:0 and 18:0. Part of the increase in diffusion can therefore be attributed to a decrease in the height of the bilayers; however, as with the case of eggPE, the percent decrease is minor compared with the percent increase in diffusion. In considering the van der Waals interactions, the removal of a lipid tail would be expected to reduce the interactions, decrease the viscosity, and increase the diffusion. In fact, calculations show that the area per lipid tail increases as the fraction of single tail lipid increases (G. Longo and I. Szleifer, personal communication, 2006), which would give rise to faster diffusion. The infrared spectroscopy measurements indicate that LPC is forming hydrogen-bonds, however, the incorporation of LPC results in an increase in diffusion; thus, relative to changes in height and van der Waals interactions the hydrogen-bond interactions are weak. Because height is a minor contribution, van der Waals interactions must be the major contribution to the increase in diffusion. Like headgroup chemistry, tail chemistry can have a large effect on lipid diffusion. These results allow us to return to the question of how much hydrogen-bonding affects lipid diffusion when eggPE is incorporated. From height and van der Waals

interactions alone large changes in diffusion can be observed; therefore it seems likely that hydrogen-bonding is a relatively minor contribution.

Lastly, the incorporation of LPE into eggPC is addressed; in this case a small decrease in diffusion was observed. Because the tail in LPE was the same length as the most abundant saturated tail in eggPC, we speculate that like eggPE, LPE increases the height of the bilayer, but only slightly. Although LPE contains the PE headgroup, which should increase the packing and therefore the van der Waals interactions, it is also missing a tail, which should decrease the van der Waals interactions. That a slight decrease in diffusion is observed indicates that the smaller headgroup is slightly more important than the removal of a tail. However, the decrease that is observed could also be attributed to the hydrogen-bonding, indicated by the infrared results, or to an increase in height. These results show that simultaneous changes to headgroup and tail chemistry can cancel out each other's effect on lipid diffusion.

Cells adjust their lipid composition for a variety of reasons, e.g., as part of cell signaling cycles, in response to external stimuli, etc. In most cases quantitative information about the changes that occur in lipid chemistry is lacking. Knowledge of these changes would be very beneficial; for instance, if the changes that occur as part of cell signaling cycles were known, it would help in understanding how all of the components work together. In the absence of this kind of information it is interesting to look at some of the common components and ask how they change membrane properties. Relating the compositions studied here to biological function we make two observations: 1) To change the diffusion by the greatest amount while making the smallest compositional change, create LPC. LPC can be made by PLA2; if a cell needs to change fluidity with a minimum of energy expenditure activating PLA2 may be a favorable pathway. 2) In red cells from normal subjects the ratio of PC/PE is ~1:1 (59). In this region diffusion is still sensitive to changes in composition; small alterations in composition could be used to change membrane fluidity to the extent that perhaps a pathway is activated.

SUMMARY AND CONCLUSIONS

The influence of lipid chemistry on membrane fluidity has been examined. It was observed that the addition of LPC and eggPE into eggPC bilayers had a significant effect, an increase and decrease, respectively, whereas the addition of LPE to eggPC bilayers had a relatively small effect, a slight decrease. The observed changes could be understood by examining the alteration in height, van der Waals interactions, and hydrogen-bonding. For all three incorporated lipids height was a significant but minor contribution as compared with the van der Waals interactions. The extent of the hydrogen-bond contribution was more difficult to ascertain; in the case of the incorporation of LPC it was minor compared to the other interactions. The large effect these other interactions had, in the case of LPC, suggests that the hydrogen-bond contribution is also relatively minor when LPE or eggPE are incorporated.

We thank the staff in the Jonathan Amy Facility for Chemical Instrumentation (JAFCI) for their help.

Jennifer S. Hovis is a recipient of a Career Award in Biomedical Sciences from Burroughs Wellcome Fund.

REFERENCES

1. Janmey, P. A., and T. P. Stossel. 1989. Gelsolin-polyphosphoinositide interaction. *J. Biol. Chem.* 264:4825–4831.
2. McCloskey, M. A., and M.-M. Poo. 1986. Contact-induced redistribution of specific membrane components: Local accumulation and development of adhesion. *J. Cell Biol.* 102:2185–2196.
3. Chan, P.-Y., M. B. Lawrence, M. L. Dustin, L. M. Ferguson, D. E. Golan, and T. A. Springer. 1991. Influence of receptor lateral mobility on adhesion strengthening between membranes containing LFA-3 and CD2. *J. Cell Biol.* 115:245–255.
4. Dustin, M. L., L. M. Ferguson, P.-Y. Chan, T. A. Springer, and D. E. Golan. 1996. Visualization of CD2 interaction with LFA-3 and determination of the two-dimensional dissociation constant for adhesion receptors in a contact area. *J. Cell Biol.* 132:465–474.
5. Pande, A. H., S. Quin, and S. A. Tatulian. 2005. Membrane fluidity is a key modulator of membrane binding, insertion, and activity of 5-lipoxygenase. *Biophys. J.* 88:4084–4094.
6. Beney, L., and P. Gervais. 2001. Influence of the fluidity of the membrane on the response of microorganisms to environmental stresses. *Appl. Microbiol. Biotechnol.* 57:34–42.
7. Gounaris, K., D. A. Mannock, A. Sen, A. P. R. Brain, W. P. Williams, and P. J. Quinn. 1983. Polyunsaturated fatty acyl residues of galactolipids are involved in the control of bilayer/non-bilayer lipid transitions in higher plant chloroplasts. *Biochim. Biophys. Acta.* 732: 229–242.
8. Sakai, A. 1987. Frost Survival of Plants: Responses and Adaptation to Freezing Stress. Springer, Berlin, Germany.
9. Murase, K., T. Fujiwara, Y. Umemura, K. Suzuki, R. Iino, H. Yamashita, M. Saito, H. Murakoshi, K. Ritchie, and A. Kusumi. 2004. Ultrafine membrane compartments for molecular diffusion as revealed by single molecule tracking. *Biophys. J.* 86:4075–4093.
10. Chang, C. H., H. Takeuchi, T. Ito, K. Machida, and S. Ohnishi. 1981. Lateral mobility of erythrocyte membrane proteins studied by the fluorescence photobleaching recovery technique. *J. Biochem. Mol. Biol. Biophys.* 90:997–1004.
11. Fujiwara, T., K. Ritchie, H. Murakoshi, K. Jacobson, and A. Kusumi. 2002. Phospholipids undergo hop diffusion in compartmentalized cell membrane. *J. Cell Biol.* 157:1071–1081.
12. Ladha, S., A. R. Mackie, L. J. Harvey, D. C. Clark, E. J. Lea, M. Brullemans, and H. Duclohier. 1996. Lateral diffusion in planar lipid bilayers: a fluorescence recovery after photobleaching investigation of its modulation by lipid composition, cholesterol, or alamethicin content and divalent cations. *Biophys. J.* 71:1364–1373.
13. Ladha, S., P. S. James, D. C. Clark, E. A. Howes, and R. Jones. 1997. Lateral mobility of plasma membrane lipids in bull spermatozoa: heterogeneity between surface domains and rigidification following cell death. *J. Cell Sci.* 110:1041–1050.
14. Lindblom, G., L. B. Johansson, and G. Arvidson. 1981. Effect of cholesterol in membranes. Pulsed nuclear magnetic resonance measurements of lipid lateral diffusion. *Biochemistry.* 20:2204–2207.
15. Smith, L. M., J. L. Rubenstein, J. W. Parce, and H. M. McConnell. 1980. Lateral diffusion of M-13 coat protein in mixtures of phosphatidylcholine and cholesterol. *Biochemistry.* 19:5907–5911.

16. Sonnleitner, A., G. J. Schutz, and T. Schmidt. 1999. Free Brownian motion of individual lipid molecules in biomembranes. *Biophys. J.* 77: 2638–2642.

17. Ratto, T. V., and M. L. Longo. 2003. Anomalous subdiffusion in heterogeneous lipid bilayers. *Langmuir.* 19:1788–1793.

18. Ratto, T. V., and M. L. Longo. 2002. Obstructed diffusion in phase-separated supported lipid bilayers: a combined atomic force microscopy and fluorescence recovery after photobleaching approach. *Biophys. J.* 83:3380–3392.

19. Adalsteinsson, T., and H. Yu. 2000. Lipid lateral diffusion in multibilayers, and in monolayers at the air/water and heptane/water interfaces. *Langmuir.* 16:9410–9413.

20. Reference deleted in proof.

21. Filippov, A., G. Oradd, and G. Lindblom. 2003. The effects of cholesterol on the laterl diffusion of phospholipids in oriented bilayers. *Biophys. J.* 84:3079–3086.

22. Kuo, A.-L., and C. G. Wade. 1979. Lipid lateral diffusion by pulsed nuclear magnetic resonance. *Biochemistry.* 18:2300–2308.

23. Oradd, G., G. Lindblom, and P. W. Westerman. 2002. Lateral diffusion of cholesterol and DMPC in a lipid bilayer measured by pfg-NMR. *Biophys. J.* 83:2702–2704.

24. Filippov, A., G. Oradd, and G. Lindblom. 2003. Influence of cholesterol and water content on phospholipid lateral diffusion in bilayers. *Langmuir.* 19:6397–6400.

25. Falck, E., M. Patra, M. Karttunen, M. T. Hyvonen, and I. Vattulainen. 2004. Lessons of slicing membranes: interplay of packing, free area, and lateral diffusion in phospholipid/cholesterol bilayers. *Biophys. J.* 87:1076–1091.

26. Niemela, P., M. T. Hyvonen, and I. Vattulainen. 2004. Structure and dynamics of sphingomyelin bilayer: insight gained through systematic comparison to phosphatidylcholine. *Biophys. J.* 87:2976–2989.

27. Filippov, A., G. Oradd, and G. Lindblom. 2004. Lipid lateral diffusion in ordered and disordered phases in raft mixtures. *Biophys. J.* 86: 891–896.

28. Scherfeld, D., N. Kahya, and P. Schwille. 2003. Lipid dynamics and domain formation in model membranes composed of ternary mixtures of unsaturated and saturated phosphatidylcholines and cholesterol. *Biophys. J.* 85:3758–3768.

29. Brian, A., and H. M. McConnell. 1984. Allogenic stimulation of cytotoxic T cells by supported planar membranes. *Proc. Natl. Acad. Sci. Unit. States Am.* 81:6159–6163.

30. Cremer, P. S., and S. G. Boxer. 1999. Formation and spreading of lipid bilayers on planar glass supports. *J. Phys. Chem. B.* 103:2554–2559.

31. Axelrod, D., D. E. Koppel, J. Schlessinger, E. Elson, and W. W. Webb. 1976. Mobility measurement by analysis of fluorescence photobleaching recovery kinetics. *Biophys. J.* 16:1055–1069.

32. Soumpasis, D. M. 1983. Theoretical analysis of fluorescence photobleaching recovery experiments. *Biophys. J.* 41:95–97.

33. Hull, M. C., L. R. Cambrea, and J. S. Hovis. 2005. Infrared spectroscopy of fluid lipid bilayers. *Anal. Chem.* 77:6096–6099.

34. Hull, M. C., D. B. Sauer, and J. S. Hovis. 2004. Influence of lipid chemistry on the osmotic response of cell membranes: effect of non-bilayer forming lipids. *J. Phys. Chem. B.* 108:15890–15895.

35. Mouritsen, O. G. 2005. Life: As a Matter of Fat. Springer-Verlag, Berlin, Germany.

36. Mantsch, H. H., and R. N. A. H. Lewis. 1991. Phospholipid phase transitions in model and biological membranes as studied by infrared spectroscopy. *Chem. Phys. Lipids.* 57:213–226.

37. Ueda, I., J. S. Chiou, P. R. Krishna, and H. Kamaya. 1994. Local anesthetics destabilize lipid membranes by breaking hydration and shell: infrared and calorimetric studies. *Biochim. Biophys. Acta.* 1190: 421–429.

38. Wong, P. T. T., and H. H. Mantsch. 1988. High pressure infrared spectroscopic evidence of water binding sites in 1,2-diacyl phospholipids. *Chem. Phys. Lipids.* 46:213–224.

39. Choi, S., W. J. Ware, S. R. Lauterbach, and W. M. Phillips. 1991. Infrared spectroscopic studies on the phosphatdylserine bilayer interacting with calcium ions: Effect of cholesterol. *Biochemistry.* 30:8563–8568.

40. McIntosh, T. J. 1996. Hydration properties of lamellar and nonlamellar phases of phosphatidylcholine and phosphatidylethanolamine. *Chem. Phys. Lipids.* 81:117–131.

41. Rand, R. P., N. Fuller, V. A. Parsegian, and D. C. Rau. 1988. Variation in hydration forces between neutral phospholipid bilayers: evidence for hydration attraction. *Biochemistry.* 27:7711–7722.

42. Sen, A., and S.-W. Hui. 1988. Direct measurement of headgroup hydration of polar lipids in inverted micelles. *Chem. Phys. Lipids.* 49: 179–184.

43. Lewis, R. N. A. H., and R. N. McElhaney. 1993. Calorimetric and spectroscopic studies of the polymorphic phase behavior of a homologous series of n-saturated 1,2-diacyl phosphatidylethanolamine. *Biophys. J.* 64:1081–1096.

44. Salgado, J., J. Villalain, and J. C. Gomez-Fernandez. 1995. Metastability of dimyristoylphosphatidylethanolamine as studied by FT-IR and the effect of alpha-tocopherol. *Biochim. Biophys. Acta.* 1239:213–225.

45. Tamm, L. K., and S. A. Tatulian. 1997. Infrared spectroscopy of proteins and peptides in lipid bilayers. *Q. Rev. Biophys.* 30:365–429.

46. Lewis, R. N., R. N. McElhaney, W. Pohle, and H. H. Mantsch. 1994. Components of the carbonyl stretching band in the infrared spectra of hydrated 1,2-diacylglycerolipid bilayers: a reevaluation. *Biophys. J.* 67: 2367–2375.

47. Galla, H.-J., W. Hartmann, U. Theilen, and E. Sackman. 1979. On two-dimensional passive random walk in lipid bilayers and fluid pathways in biomembranes. *J. Membr. Biol.* 48:215–236.

48. MacCarthy, J. E., and J. K. Kozak. 1982. Lateral diffusion in fluid systems. *J. Chem. Phys.* 77:2214–2216.

49. Edholm, O., and J. F. Nagle. 2005. Areas of molecules in membranes consisting of mixtures. *J. Phys. Chem. B.* 89:1827–1832.

50. Falck, E., M. Patra, M. Karttunen, M. T. Hyvonen, and I. Vattulainen. 2005. Response to comment by Almeida et al.: free area theories for lipid bilayers-predictive or not? *Biophys. J.* 89:745–752.

51. Saffman, P. G., and M. Delbruck. 1975. Brownian motion in biological membranes. *Proc. Natl. Acad. Sci. Unit. States Am.* 72:3111–3113.

52. Israelachvili, J. 1992. Intermolecular and Surface Forces. Academic Press, New York.

53. Leekumjorn, S., and A. K. Sum. 2006. Molecular simulation study of structural and dynamic properties of mixed DPPC/DPPE bilayers. *Biophys. J.* 90:3951–3965.

54. De Young, L. R., and K. A. Dill. 1988. Solute partitioning into lipid bilayer-membranes. *Biochemistry.* 27:5281–5289.

55. Petrache, H. I., K. C. Tu, and J. F. Nagle. 1999. Analysis of simulated NMR order parameters for lipid bilayer structure determination. *Biophys. J.* 76:2479–2487.

56. Petrache, H. I., S. W. Dodd, and M. F. Brown. 2000. Area per lipid and acyl length distributions in fluid phosphatidylcholines determined by H-2 NMR spectroscopy. *Biophys. J.* 79:3172–3192.

57. Schindler, H., and J. Seelig. 1975. Deuterium order parameters in relation to thermodynamic properties of a phospholipid bilayer - statistical mechanical interpretation. *Biochemistry.* 14:2283–2287.

58. de Vries, A. H., A. E. Mark, and S. J. Marrink. 2004. The binary mixing behavior of phospholipids in a bilayer: a molecular dynamics study. *J. Phys. Chem. B.* 108:2454–2463.

59. Dodge, J. T., and G. B. Phillips. 1967. Composition of phospholipids and of phospholipid fatty acids and aldehydes in human red cells. *J. Lipid Res.* 8:667–675.